A DISTURBANCE BASED CONTROL/STRUCTURE DESIGN ALGORITHM

Mark D. McLaren [1]
Gary L. Slater [2]

Department of Aerospace Engineering and Engineering Mechanics
ML # 70, University of Cincinnati, Cincinnati, OH 45221

1 Introduction

In the past, the structure and its control system have been designed independently. Structural design and optimization, and control system design and optimization, have each been areas of separate research, each progressing vigorously along its own path. However, spurred on by recent proposals of new, large, highly constrained space structures, the question has arisen as to whether an integrated structural/control design procedure might not be more appropriate. The first papers actively investigating the question of simultaneous structure and control design began appearing in the literature around 1983 [1,2,3]. Since then, there has been a growing interest in this subject from other authors, although the field itself is still in relative infancy. Using a conventional design approach for a controlled structure, one would first optimize the structure alone, then design a control system for this baseline structure. This process may then be iterated until both the structure and control system meet necessary constraints and objectives.

Some authors ([4,5,6,7], for example) take a "classical" approach to the simultaneous structure/control optimization by attempting to simultaneously minimize the *weighted* sum of the total mass and a quadratic form, subject to all of the structural and control constraints. In this paper, the optimization will be based on the dynamic response of a structure to an external unknown stochastic disturbance environment [8]. Such a "response to excitation approach" is common to both the structural and control design phases, and hence represents a more natural control/structure optimization strategy than relying on artificial and vague control penalties. The design objective is to find the structure and controller of minimum mass such that all the prescribed constraints are satisfied.

Two alternative solution algorithms will be presented which have been applied to this problem. Each algorithm handles the optimization strategy and the imposition of the nonlinear constraints in a different manner. Two controller methodologies, and their effect on the solution algorithm, will be considered. These are full state feedback and direct output feedback, although the problem formulation is not restricted solely to these forms of controller. In fact, although full state feedback is a popular choice among researchers in this field (for resons that will become apparent), its practical application is severely limited. The controller/structure interaction is inserted by the imposition of appropriate closed-loop constraints, such as closed-loop output response and control effort constraints. Numerical results will be obtained for a representative flexible structure model to illustrate the effectiveness of the solution algorithms.

2 General Problem Formulation

The integrated control/structure design optimization problem can be stated as follows: find the vector of structural and controller parameters that minimizes the mass of the structure subject to a set of prescribed stochastic disturbances, with limitations on the available control energy and on a set of allowable output responses. This can be written in the form of a nonlinear mathematical programming problem as

[1] Graduate Student
[2] Professor

Minimize, with respect to $\boldsymbol{p}$, the weight $J(\boldsymbol{p})$, subject to

$$\boldsymbol{g}(\boldsymbol{p}) \leq 0$$

$$\dot{\boldsymbol{x}} = F\boldsymbol{x} + G\boldsymbol{u} + G_w\boldsymbol{w}$$

$$g_{cc_i} = \frac{\mathrm{E}[\boldsymbol{u}_i^T R_i \boldsymbol{u}_i]}{\beta_i^2} - 1 \leq 0 \qquad \text{for } i = 1, \ldots, n_\beta \tag{1}$$

$$g_{oc_i} = \frac{\mathrm{E}[\boldsymbol{y}_{d_i}^T W_i \boldsymbol{y}_{d_i}]}{\alpha_i^2} - 1 \leq 0 \qquad \text{for } i = 1, \ldots, n_\alpha$$

$$\boldsymbol{y}_{d_i} = H_{d_i}\boldsymbol{x} \qquad \text{for } i = 1, \ldots, n_\alpha$$

$$\boldsymbol{p}_\ell \leq \boldsymbol{p} \leq \boldsymbol{p}_u$$

where

$\boldsymbol{p}$	is an N-vector of design variables,
$\boldsymbol{g}$	is an m-vector of structural constraints,
$\boldsymbol{x}$	is an n-vector of state variables,
$\boldsymbol{u}$	is an n_u-vector of control forces,
$\boldsymbol{w}$	is an n_w-vector of stochastic disturbances,
F	is the $(n \times n)$ matrix containing the system dynamics,
G	is the $(n \times n_u)$ matrix containing information on the locations and orientations of the actuators,
G_w	is the $(n \times n_w)$ matrix containing information on the points of application and orientation of the disturbances,
g_{cc_i}	is the i^{th} control effort constraint cost function,
$\boldsymbol{u}_i$	is the n_{u_i}-order partition of $\boldsymbol{u}$ representing the control forces involved in g_{cc_i},
β_i	is the maximum allowable value of the i^{th} expected control effort function $\mathrm{E}[\boldsymbol{u}_i^T R_i \boldsymbol{u}_i]$,
R_i	is an $(n_{u_i} \times n_{u_i})$ control force weighting matrix,
g_{oc_i}	is the i^{th} output response constraint cost function,
α_i	is the maximum allowable value of the i^{th} expected output response function $\mathrm{E}[\boldsymbol{y}_{d_i}^T W_i \boldsymbol{y}_{d_i}]$,
W_i	is an $(n_{d_i} \times n_{d_i})$ output response weighting matrix,
$\boldsymbol{y}_{d_i}$	is the i^{th} design output n_{d_i}-vector,
H_{d_i}	is an $(n_{d_i} \times n)$ matrix giving the relationship between the state variables and $\boldsymbol{y}_{d_i}$,
$\boldsymbol{p}_\ell$	is an N-vector of minimum design variable values, and
$\boldsymbol{p}_u$	is an N-vector of maximum design variable values.

The side constraints are the strict bounds $\boldsymbol{p}_\ell$ and $\boldsymbol{p}_u$ on the design variables, and are vector inequalities that are imposed element by element. These design variable bounds are not included explicitly as constraints in the problem formulation. Note that the structural weight and the structural constraints $\boldsymbol{g}$ will in general not be functions of the controller design variables unless the controller mass is included in the design. Note also that g_{cc_i} is a weighted mean square control effort, and g_{oc_i} is a weighted mean square output response. Multiple output response constraints are allowed, although only one of these will in general be active at the optimum design. However, all of the control effort constraints will generally be active at the optimum design.

In this work $\boldsymbol{w}$ is a zero mean Gaussian white noise disturbance with covariance X_w. The structure will respond to this disturbance with some transient behaviour, in addition to a steady-state response. It seems

reasonable to optimize the structure for the steady-state response to the disturbance rather than the transient response because the transient behaviour will normally be of secondary importance to the response objectives (such as long term pointing accuracy). Also, for steady state optimization, the differential equation constraint (state equation) can be replaced with a steady state covariance equation, so that the control effort and output response constraints may be recast in terms of this covariance. Therefore the two-point boundary value problem is eliminated and the numerical solution of the problem is significantly simplified.

2.1 Full State Feedback Control

The simplest form of feedback control is to feedback the entire state vector, with $\boldsymbol{u} = -K\boldsymbol{x}$, where K is the $(n_u \times n)$ state feedback gain matrix. The controller design variables for this case will be the $n_u n$ elements of K. Substituting this control into the state equation, and assuming that the disturbance $\boldsymbol{w}$ is zero mean Gaussian white noise, the state covariance matrix X for this case can be found from the Lyapunov equation

$$F_{cl}X + XF_{cl}^T + G_w X_w G_w^T = 0 \tag{2}$$

where $F_{cl} = (F - GK)$ is the *stable* closed-loop dynamical matrix for the full state feedback case, $X = \mathrm{E}[\boldsymbol{x}\boldsymbol{x}^T]$ is the $(n \times n)$ symmetric state covariance matrix, and $X_w = \mathrm{E}[\boldsymbol{w}\boldsymbol{w}^T]$ is the $(n_w \times n_w)$ symmetric covariance matrix for the stochastic disturbances.

Expressions for the controller constraints in terms of this covariance matrix can then be obtained as

$$g_{cc_i} = \frac{\mathrm{tr}[K_i^T R_i K_i X]}{\beta_i^2} - 1 \qquad \text{for } i = 1, \ldots, n_\beta \tag{3}$$

$$g_{oc_i} = \frac{\mathrm{tr}[H_{d_i}^T W_i H_{d_i} X]}{\alpha_i^2} - 1 \qquad \text{for } i = 1, \ldots, n_\alpha \tag{4}$$

where K_i is the $(n_{u_i} \times n)$ partition of K corresponding to $\boldsymbol{u}_i$. It is assumed that the $\boldsymbol{u}_i$ are independent, and that $\boldsymbol{u}$ and K are ordered as

$$\boldsymbol{u}^T = \left[\begin{array}{cccc} \boldsymbol{u}_1^T & \boldsymbol{u}_2^T & \cdots & \boldsymbol{u}_{n_\beta}^T \end{array}\right], \qquad K^T = \left[\begin{array}{cccc} K_1^T & K_2^T & \cdots & K_{n_\beta}^T \end{array}\right] \tag{5}$$

Note that $\sum_{i=1}^{n_\beta} n_{u_i} = n_u$, and that the columns of G can be interchanged to force condition (5) to be satisfied. Using full state feedback, the first-order necessary (Kuhn-Tucker) conditions for optimality can be analytically solved to give [8]

$$K = R^{-1}G^T\Lambda_x, \qquad \text{where} \qquad F^T\Lambda_x + \Lambda_x F - \Lambda_x G R^{-1} G^T \Lambda_x + W = 0 \tag{6}$$

and where R and W are respectively the $(n_u \times n_u)$ and $(n \times n)$ matrices defined as

$$R = \mathrm{diag}\left\{\left(\frac{\lambda_{u_i}}{\beta_i^2}\right) R_i\right\}, \qquad W = \sum_{i=1}^{n_\alpha} \left(\frac{\lambda_{y_i}}{\alpha_i^2}\right) H_{d_i}^T W_i H_{d_i}. \tag{7}$$

The variables λ_{u_i} and λ_{y_i} come from the Kuhn-Tucker conditions, and are the Lagrange multipliers associated with the i^{th} control effort and output response constraints respectively.

Equations (6) define the solution to the optimal control problem

$$\min\ J_c = \int_0^\infty \left[\boldsymbol{x}^T W \boldsymbol{x} + \boldsymbol{u}^T R \boldsymbol{u}\right] \mathrm{dt} \tag{8}$$

where K is the optimal steady-state gain matrix, and Λ_x is the steady-state solution to the associated Riccati equation. Although this LQR property only holds true at the optimum point, it is computationally convenient to assume that at every point in the design cycle, the control design variables will be found as the solution to the optimal control problem (8). Therefore, the numerical optimization problem can be reduced to optimization over just the structural design variables, along with an optimal control problem solution which will be a function of the Lagrange multiplier vectors $\boldsymbol{\lambda}_u$ and $\boldsymbol{\lambda}_y$. The immediate benefit of this is a reduced dimensionality nonlinear programming problem. In addition, since the regulator solutions always give a stable closed-loop

system, no explicit check must be performed on the system stability during the solution procedure. The LQR assumption in this proble formulation is similar to the approach taken in [9,10], and others, where R and W are fixed, and not chosen to satisfy the constraints.

2.2 Direct Output Feedback Control

For most real systems, the state vector will be very large, and the use of full state feedback would result in a controller of unacceptably high dimension, assuming additionally that the entire state is available. However, usually only a small subset of the system states will be available to the designer, in the form of the output measurement vector. These can include actual system states along with linear combinations of the system states, in the form $\boldsymbol{y} = H\boldsymbol{x}$, where $\boldsymbol{y}$ is the n_y-vector of outputs and H is the $(n_y \times n)$ output matrix giving the relationship between the outputs and the system states. If these output states are to be used in the feedback loop, the resulting control is termed direct output feedback, with the control forces defined to be $\boldsymbol{u} = -K\boldsymbol{y}$, where K is the $(n_u \times n_y)$ output feedback gain matrix. In this case, the controller design variables will be the $n_u n_y$ elements of K.

Substituting this control into the state equation, the state covariance matrix X for this case can be found as the solution to the same Lyapunov equation (2), except that now the closed-loop dynamics are given by $F_{cl} = (F - GKH)$. Note that since K does not satisfy any special conditions (such as the LQR conditions), the closed-loop system F_{cl} is not guaranteed to be stable for any K. If F_{cl} is unstable at any stage in the solution procedure, the covariance matrix X cannot be found from equation (2). Therefore, for this case, hard constraints on the closed-loop system eigenvalues must be imposed at every step in the design proceedure. "Hard" in this sense means that special precautions must be taken in the solution procedure such that these constraints can never be violated.

Expressions for the controller constraints for direct output feedback in terms of the covariance matrix can then be found to be

$$g_{cc_i} = \frac{\mathrm{tr}[H^T K_i^T R_i K_i H X]}{\beta_i^2} - 1 \qquad \text{for } i = 1, \ldots, n_\beta \tag{9}$$

$$g_{oc_i} = \frac{\mathrm{tr}[H_{d_i}^T W_i H_{d_i} X]}{\alpha_i^2} - 1 \qquad \text{for } i = 1, \ldots, n_\alpha \tag{10}$$

3 Solution Algorithms

In the general problem formulation presented in the previous section, the constraint functions are generally highly nonlinear implicit functions of the design variables. Solution of this problem could be attempted by the direct application of nonlinear programming techniques; that is, using the exact functional expressions for the constraints. However, this approach quickly becomes computationally very expensive as the dimensionality increases since the full objective and constraint functions must be evaluated at every step, and their respective gradients at most, if not all, steps thoughout the design procedure. Such evaluations tend to be computationally very expensive.

Approximation techniques, where the implicit nonlinear problem is replaced by a sequence of explicit approximate (although not necessarily linear) problems, have been shown to yield efficient and powerful algorithms for structural design optimization (see, for example, [11,12]). In this paper, two solution techniques based on approximation techniques will be tested on the integrated control/structure design optimization problem. The methods will be compared with respect to the ease of use, generality of application, and numerical robustness to changes in move-limits and other solution parameters.

3.1 Sequential Nonlinear Approximations

In this method, the fully constrained nonlinear optimization problem is solved by the iterative construction and numerical solution of a sequence of explicit approximate problems. The approximate problems are first-order Taylor's series expansions (with respect to either the inverse design variables ([13], for example), or with respect to hybrid design variables [14]) of the objective and constraint functions. Depending on the intermediate

variables chosen, the approximate functions may still be nonlinear functions of the design variables. Therefore, the numerical solution is accomplished using a mathematical programming code, specifically the modified method of feasible directions as implemented in ADS [15].

The solution process begins with some initial structure, which is analyzed using the finite element technique. At this point, the gradients of the active constraint set are evaluated, and the approximate problem is formed, with respect to the current design. Expressions for the gradients of all constraints considered can be evaluated analytically. The approximate problem is solved with ADS using an active constraint set strategy to reduce the dimensionality of the approximate problem by deleting the inactive constraints. Move-limits on the design variables are imposed during the solution to ensure that the design remains within the region for which the approximation functions are of acceptable quality. The choice of move-limits and how they change can have a significant effect on convergence, and will often be determined from numerical experience with the particular problem at hand.

After the solution of the approximate problem, the structure and its control system are deemed optimal if a convergence test on either the absolute or relative objective function change over a specified number of successive global iterations is satisfied. Otherwise, the objective and active constraint gradients are evaluated for the new design, a new approximate problem formed, and the process above is repeated in an iterative manner. The solution procedure ends when the design variables converge, or when the number of iterations exceeds some preset maximum.

Scaling the structure and controller to the closest constraint surface may be possible in some cases, because of the special assumed form of the controller. Scaling to structural constraints has been performed in other work (see [16]) and will not be covered here. If full state feedback is used, it is possible and practical to scale the structure to the closest control effort constraint and closest output response constraint simultaneously. The variables with which the structure is scaled are the structural design variables (elemental areas or thicknesses), and the Lagrange multipliers associated with the two controller constraints λ_u and λ_y (where for clarity, and without loss of generality, the subscripts on the λ's that refer to the particular control effort or output response constraints under consideration have been dropped).

Note that changing the values of λ_u and λ_y cannot independently change the values of $u_{ms} = \mathrm{tr}(K^T R K X)$ and $y_{ms} = \mathrm{tr}(H_d^T W H_d X)$, because in the LQR problem, only the ratio of λ_u to λ_y is important. One can choose the ratio (λ_u/λ_y) to satisfy one of the control constraints — say u_{ms}. Then y_{ms} will not in general be satisfied. Suppose y_{ms} is too large (i.e. $y_{ms} > \alpha^2$) at the particular point where u_{ms} is satisfied. Then the *only* way one can satisfy the y_{ms} constraint is to increase the sizes of at least some of the structural members. This seems reasonable because if the control constraints could be satisfied by simply choosing appropriate controller parameters, then there would be no interaction between structural optimization and controller optimization. Intuitively, it can be seen that this is not the case. Note that each member of the structure will be scaled by the same amount to fulfill our goals. Obviously, this method is not absolutely mandated, and some other approach could be used where the design variables are not scaled equally. However, this would then be *resizing* rather than *scaling*, a process normally left to the nonlinear programming algorithm.

The final scaling aim is to set $u_{ms} = \beta^2$ and $y_{ms} = \alpha^2$. To perform the scaling, it is assumed that, at iteration i, the values $(u_{ms})_i$ and $(y_{ms})_i$ will change, as a result of changes to $(\lambda_u)_i$ and the $(p_j)_i$, according to the equations

$$\frac{(u_{ms})_{i+1}}{(u_{ms})_i} = \Delta_{i+1}^{a_i} \delta_{i+1}^{b_i}, \qquad \frac{(y_{ms})_{i+1}}{(y_{ms})_i} = \Delta_{i+1}^{c_i} \delta_{i+1}^{d_i} \tag{11}$$

where a_i, b_i, c_i and d_i are constants, and where

$$\Delta_{i+1} = \frac{(\lambda_u)_{i+1}}{(\lambda_u)_i}, \qquad \delta_{i+1} = \frac{(p_j)_{i+1}}{(p_j)_i} \tag{12}$$

If initial (educated) guesses for these constants can be made, they can be updated in an adaptive manner during the scaling proceedure.

Move-limits are imposed on the design variables during each approximate problem solution. This is done in an attempt to restrain the design variables to a region in which the explicit function approximations remain reasonably accurate. However, deciding how to impose these move-limits is a non-trivial task. The local curvature of the design space (i.e. how nonlinear are the actual constraint surfaces in the region about the expansion point of the approximations) will determine the move-limits, with more strict move-limits applied in regions

of high curvature, and less strict move-limits imposed in regions of low curvature. Since second-derivative information is required to estimate curvatures, and since such evaluations are very expensive computationally, imposing move-limits is usually reduced to an art based on past experience. Quasi-Newton methods obtain the second derivatives using only first derivative information, however, these methods typically take N iterations to fill the Hessian, and can be very costly if N is large.

For the purpose of this work, a move-limits factor γ is imposed in an exponential form. If the current design variable and approximation expansion vector is $\boldsymbol{p}$, then the upper and lower bounds on the design variables for the current approximate problem are defined as

$$\boldsymbol{p}_u = \gamma \boldsymbol{p}, \qquad \boldsymbol{p}_\ell = \frac{1}{\gamma}\boldsymbol{p} \tag{13}$$

where $\gamma \geq 1$. The limits specified in equation (13) must be imposed element by element. Note that since the design variables in this example will be structural design variables only, they are restricted to be positive. Obviously, equation (13) must be modified if the design variables can be negative. The exponential form of the move-limit factor is defined by the particular choice of γ_{min} and γ_{max} (typically 1.2 and 1000 respectively in this work).

3.2 Continuation and Sequential Linear Programming

The complex nature of the constraint functions in the nonlinear optimization problem, especially the controller constraints, leads to various convergence problems in the context of a classical gradient based nonlinear programming code such as ADS. As the problem dimensionality increases, convergence will usualy become increasingly difficult to accomplish, as step sizes reduce to satisfy the local linearity assumptions inherent in gradient based solution techniques. Another method for the solution of mathematical programming problems that has recently become popular is the use of continuation methods to impose nonlinear constraints coupled with sequential linear programming (SLP) [17,18]. The continuation procedure is a conceptually simple method of applying restrictive constraints gradually from less restrictive ones, which replaces the most demanding constraint functions of the form $g(\boldsymbol{p}) \leq 0$, by a set of neighbouring constraint functions $\mathcal{G}_i$, defined by

$$\mathcal{G}_i(\boldsymbol{p}_i, \gamma_i) = g(\boldsymbol{p}_i) - (1-\gamma_i) g(\boldsymbol{p}_0) \leq 0 \qquad \text{for } i = 0, \ldots, M \tag{14}$$

where $\boldsymbol{p}_0$ is the arbitrarily chosen initial design point, and γ_i is a continuation parameter satisfying

$$0 = \gamma_0 \leq \gamma_1 \leq \cdots \leq \gamma_M = 1 \tag{15}$$

Note that for $\gamma_0 = 0$, when $\boldsymbol{p} = \boldsymbol{p}_0$, the new constraint function $\mathcal{G}_0$ is identically satisfied. If convergence is acheived for $\gamma = 1$, then the original constraints will be recovered in M steps. The step size $\Delta\gamma = \gamma_i - \gamma_{i-1}$ (and hence M), can be chosen small enough so that assumptions on local linearity can be almost arbitrarily satisfied.

Linear Programming (LP) methods are a powerful approach to handling a large number of locally linear constraints, and due to the wide availability of very efficient LP codes, are an attractive alternative to nonlinear programming methods. The neighbouring problems generated by the continuation procedure can be written in the form

$$\text{Minimize } J(\boldsymbol{p}_i), \text{ subject to } \mathcal{G}_i(\boldsymbol{p}_i, \gamma_i) \leq 0 \tag{16}$$

To transform these equations into a linear programming problem, the equations are linearized about the current point $\boldsymbol{p}_i$, and move-limits on the maximum parameter changes allowable locally are imposed. Expanding the objective and constraint equations in (16) to first order in a Taylor's series expansion about $\boldsymbol{p}_i$ gives the locally linearized problems in linear programming form as

$$\text{Minimize, with respect to } \Delta \boldsymbol{p}_i,\ \Delta J_i = \left[\frac{\partial J}{\partial \boldsymbol{p}}\right]_{\boldsymbol{p}_i} \Delta \boldsymbol{p}_i, \text{ subject to}$$

$$\left[\frac{\partial \mathcal{G}_i(\boldsymbol{p}_i, \gamma_i)}{\partial \boldsymbol{p}}\right]_{\boldsymbol{p}_i} \Delta \boldsymbol{p}_i + \boldsymbol{g}(\boldsymbol{p}_i) - (1-\gamma_i)\boldsymbol{g}(\boldsymbol{p}_0) \leq 0 \tag{17}$$

$$-\boldsymbol{\epsilon} \leq \Delta \boldsymbol{p}_i \leq \boldsymbol{\epsilon}$$

for $i = 0, \ldots, (M-1)$. All elements of $\boldsymbol{\epsilon}$ are assumed positive, and the vector inequality is imposed element by element.

The algorithm begins with an initial structure, which is analyzed using the finite element technique. The initial problem ($\gamma_0 = 0$) is solved, and the continuation parameter γ is incremented from $\gamma_0 = 0$ by $\Delta\gamma$ to γ_1. Note that if initially $K = 0$, so that the control effort allowed for the initial local problem is zero, this initial problem becomes a pure structural optimization subject to the dynamic output repsonse constraints. The increment $\Delta\gamma$ is set by an a priori choice of M, the number of continuation steps, although $\Delta\gamma$ need not be constant throughout the solution procedure. Successful implementation of the continuation method has been reported when $\Delta\gamma$ was chosen as initially quite small and increased to a larger value during the solution [18]. The choice of $\Delta\gamma$ is closely coupled with the choice of the nominal design variable move limit vector $\boldsymbol{\epsilon}_0$. There is in fact a tradeoff between the satisfaction of the local linearity assumption through $\boldsymbol{\epsilon}$, and the ability to converge to the neighbouring problem through $\Delta\gamma$. Usually, for each particular problem, some numerical trial and error will be required to find those values of $\boldsymbol{\epsilon}_0$ and $\Delta\gamma$ that yield an efficient solution technique.

The gradients of the objective and constraint functions are calculated at the current design, and then the associated linear programming problem (17) is solved by a linear programming code. In this work, the linear programming routine E04MBF from NAGLIB (National Algorithms Group LIBrary) was used, although other routines inserted at this point should provide the same solution. Since the local linearity assumption will never be exactly satisfied, the actual constraint values at the new point, specified by the solution to the linear programming problem, will be different than that predicted. Therefore, the constraints $\mathcal{G}_i$ may not be satisfied following the linear programming solution step.

Since a converged subproblem solution is required before increasing the continuation parameter, this local problem is iterated locally until convergence is obtained. At each local iteration, new gradients are calculated, and the move limits on the design variables are reduced so that $\boldsymbol{\epsilon} = c\boldsymbol{\epsilon}_0$, where a value of $c = 0.75$ was used in this work. If convergence to the local problem does not occur within 15 iterations (where move limits are about 1% of their nominal values), the move limits are increased to their nominal values $\boldsymbol{\epsilon}_0$, and the local iterations are repeated. Numerical experience with this algorithm has shown that this procedure is flexible enough numerically so that converged subproblem solutions can be obtained in a reasonable number of local iterations, as long as the neighbouring problems are "close enough". Practically, this means that either the constraint values of the initial system should be "close" to their final desired values, or that M should be large. Once the local problem has been solved, the continuation parameter γ is incremented, and the new local problem solved as before. At the M^{th} continuation step, $\gamma = 1$ and the original problem is recovered, so that the solution to the M^{th} local problem is the solution to the original problem.

If closed-loop stability constraints are violated at any stage in the solution procedure, these must be imposed immediately. To achieve this, it is possible to employ a method that never requires the calculation of the closed-loop eigenvalue derivatives, saving considerable computational expense. Of course, if in addition to overall stability there are constraints on closed-loop damping ratios or bandwidth, then the evaluation of the closed-loop eigenvalue derivative may be necessary at some point. The method used in this paper is to simply bisect $\Delta\boldsymbol{p}_i$ and perform another analysis until a stable system configuration is obtained.

4 Gradient Analysis

For the numerical optimization procedure to be practical, especially as the dimensionality increases to realistic structures, it is essential that it be possible to evaluate the first-order sensitivities of the complex constraint functions in an efficient manner. The objective function (the weight) is a linear function of the finite element

thicknesses and/or cross sectional areas (for truss type finite elements), so that its gradient is easy to calculate at any point in the design space.

4.1 Gradients for the case of Full State Feedback Control

The gradients of the controller constraints with respect to a structural design variable p_j are given by

$$\frac{\partial g_{cc_i}}{\partial p_j} = \frac{1}{\beta_i^2}\mathrm{tr}\left[\left(\frac{\partial K_i^T}{\partial p_j}R_iK_i + K_i^TR_i\frac{\partial K_i}{\partial p_j}\right)X + \mathcal{P}_i\mathcal{H}_j\right] \tag{18}$$

$$\frac{\partial g_{oc_i}}{\partial p_j} = \frac{1}{\alpha_i^2}\mathrm{tr}\left[\left(\frac{\partial H_{d_i}^T}{\partial p_j}W_iH_{d_i} + H_{d_i}^TW_i\frac{\partial H_{d_i}}{\partial p_j}\right)X + \mathcal{Q}_i\mathcal{H}_j\right] \tag{19}$$

where $\mathcal{P}_i$, $\mathcal{Q}_i$, and $\mathcal{H}_j$ are evaluated using the following set of equations:

$$F_{cl}^T\mathcal{P}_i + \mathcal{P}_iF_{cl} + K_i^TR_iK_i = 0 \tag{20}$$

$$F_{cl}^T\mathcal{Q}_i + \mathcal{Q}_iF_{cl} + H_{d_i}^TW_iH_{d_i} = 0 \tag{21}$$

$$\mathcal{H}_j = \left[\frac{\partial F_{cl}}{\partial p_j}X + X\frac{\partial F_{cl}^T}{\partial p_j} + \frac{\partial G_w}{\partial p_j}X_wG_w^T + G_wX_w\frac{\partial G_w^T}{\partial p_j}\right] \tag{22}$$

$$\frac{\partial F_{cl}}{\partial p_j} = \left(\frac{\partial F}{\partial p_j} - \frac{\partial G}{\partial p_j}K - G\frac{\partial K}{\partial p_j}\right) \tag{23}$$

$$\frac{\partial K}{\partial p_j} = R^{-1}\left[\frac{\partial G^T}{\partial p_j}\Lambda_x + G^T\frac{\partial \Lambda_x}{\partial p_j}\right] \tag{24}$$

$$F_{cl}^T\frac{\partial \Lambda_x}{\partial p_j} + \frac{\partial \Lambda_x}{\partial p_j}F_{cl} = -\left[\left(\frac{\partial F}{\partial p_j} - \frac{\partial G}{\partial p_j}K\right)^T\Lambda_x + \Lambda_x\left(\frac{\partial F}{\partial p_j} - \frac{\partial G}{\partial p_j}K\right) + \frac{\partial W}{\partial p_j}\right] \tag{25}$$

$$\frac{\partial W}{\partial p_j} = \sum_{i=1}^{n_\alpha}\left(\frac{\lambda_{y_i}}{\alpha_i^2}\right)\left(\frac{\partial H_{d_i}^T}{\partial p_j}W_iH_{d_i} + H_{d_i}^TW_i\frac{\partial H_{d_i}}{\partial p_j}\right) \tag{26}$$

Note that gradients with respect to controller design variables need not be evaluated since these design variables were effectively removed from the optimization problem by the LQR constraint.

4.2 Gradients for the case of Direct Output Feedback Control

The gradients of the controller constraints with respect to a structural design variable p_j are given by

$$\frac{\partial g_{cc_i}}{\partial p_j} = \frac{1}{\beta_i^2}\mathrm{tr}\left[\left(\frac{\partial H^T}{\partial p_j}K_i^TR_iK_iH + H^TK_i^TR_iK_i\frac{\partial H}{\partial p_j}\right)X + \mathcal{Y}_i\mathcal{N}_j\right] \tag{27}$$

$$\frac{\partial g_{oc_i}}{\partial p_j} = \frac{1}{\alpha_i^2}\mathrm{tr}\left[\left(\frac{\partial H_{d_i}^T}{\partial p_j}WH_{d_i} + H_{d_i}^TW_i\frac{\partial H_{d_i}}{\partial p_j}\right)X + \mathcal{Z}_i\mathcal{N}_j\right] \tag{28}$$

where $\mathcal{Y}_i$, $\mathcal{Z}_i$, and $\mathcal{N}_j$ are evaluated using the following set of equations:

$$F_{cl}^T\mathcal{Y}_i + \mathcal{Y}_iF_{cl} + H^TK_i^TR_iK_iH = 0 \tag{29}$$

$$F_{cl}^T\mathcal{Z}_i + \mathcal{Z}_iF_{cl} + H_{d_i}^TW_iH_{d_i} = 0 \tag{30}$$

$$\mathcal{N}_j = \left[\frac{\partial F_{cl}}{\partial p_j}X + X\frac{\partial F_{cl}}{\partial p_j}^T + \frac{\partial G_w}{\partial p_j}X_wG_w^T + G_wX_w\frac{\partial G_w^T}{\partial p_j}\right] \tag{31}$$

$$\frac{\partial F_{cl}}{\partial p_j} = \left(\frac{\partial F}{\partial p_j} - \frac{\partial G}{\partial p_j}KH - GK\frac{\partial H}{\partial p_j}\right) \tag{32}$$

The gradients of the controller constraints with respect to the elements of the gain matrix K can be written in matrix expression form as

$$\frac{\partial g_{cc_i}}{\partial K} = \frac{2}{\beta_i^2}\left[\{\mathcal{R}_i K H - G^T \mathcal{Y}_i\}\, X H^T\right] \tag{33}$$

$$\frac{\partial g_{oc_i}}{\partial K} = -\frac{2}{\alpha_i^2}\left[G^T \mathcal{Z}_i X H^T\right] \tag{34}$$

where, for scalar s and matrix A with elements a_{ij}, $\left[\frac{\partial s}{\partial A}\right]_{ij} = \frac{\partial s}{\partial a_{ij}}$, and where

$$\mathcal{R}_i = \text{diag}\ \{0 \cdots 0\ \ R_i\ \ 0 \cdots 0\ \}_{(n_u \times n_u)} \tag{35}$$

Note that the R_i in equation (35) is of order $(n_{u_i} \times n_{u_i})$, and is in the i^{th} diagonal block of $\mathcal{R}_i$.

5 Example: The DRAPER I Teterahedral Truss Structure

The DRAPER I structure [19] is a tetrahedral truss attached to the ground by three right-angled bipods, as shown in Figure 1. Although attached to the ground, this model will act as a typical flexible structure pointing subsystem (e.g. antenna, radar, optical) attached to a rigid core. Any motion would then be with respect to this rigid core, and transmit forces to it. Consequently, this model has no rigid body degrees of freedom. The finite element model has 12 truss elements, since the joints are pinned and transmit no moments. There are four nodes that are free to move in all directions, so the model contains 12 degrees of freedom. The structural design variables are the cross-sectional areas of each of the 12 truss elements. Since there are 12 degrees of freedom in the model for this structure, the state-space model will be 24^{th} order. There will be 6 inputs corresponding to the 6 legs of the structure, and a varying number of outputs, depending on the problem at hand.

For the purposes of this work, material parameters of $\rho = 0.1$ lb/in and $E =$ Young's Modulus $= 20$ kpsi were used. The dimensional values E and ρ were chosen to give initial numerical values of structural frequencies for the dimensional model roughly comparable to those of the non-dimensional model. The model contains no nonstructural mass. Elements 7 through 12, the three right-angled bipods, take on the duties of force actuators (and possibly colocated velocity and/or displacement sensors). Only one output response constraint is defined ($n_\alpha = 1$), with the design output vector y_d representing the line-of-sight error of the top vertex [(x, y) displacements of vertex 1]. The disturbances, labelled w_1 and w_2 in Figure 2, are assumed to be independent, zero mean, Gaussian disturbances with intensity 1.0.

The damping added to the state space system will depend on the state space realization used. For cases where a realization based on physical variables is used, the damping matrix C is formed to be $C = 0.1M + 0.001K_s$, For cases where a realization based on modal variables was used, the damping ratio of each mode was specified to be 0.1% of the modal frequencies during the formation of the state matrices. The weighting matrices R and W are set to the identity matrices, so that equal weighting is given to all components of $\boldsymbol{u}$ and $\boldsymbol{y_d}$. The minimum cross-sectional areas for all elements was specified as 0.1 in^2. For this problem, no static structural constraints were specified in this model of the DRAPER I structure, the intent being to investigate the effect of the closed-loop controller constraints on the structural design optimization.

5.1 Full State Feedback Control

In this section, the sequential nonlinear approximations solution algorithm, with the addition of the scaling procedure outlined in Section 3.1, is applied to the full state feedback control of the DRAPER I structure. The effect of the scaling procedure used here can be determined by applying the sequential approximations algorithm in the form of a direct output feedback problem with $H = I$ with no scaling assumed. The continuation solution algorithm is also best handled in the form of a direct output feedback problem since no special scaling is assumed. Both solution algorithms applied to the case of full state feedback are discussed in Section 5.2, where direct output feedback control is considered. For brevity, only limited results for both

controller methodologies are presented in this paper, but a full discussion of this example can be found in reference [20].

Runs were made optimizing the DRAPER I structure using an inverse design variable approximation for all constraint functions. The initial structure was defined with all structural design variables set at 10 in^2, and with the Lagrange multipliers λ_u and λ_y set at 1.0. This set of initial conditions will be termed the symmetric set of initial conditions, for they specify a structure with a number of vibrational modes of the same frequency (repeated eigenvalues). A range of allowable expected output response (α^2) of 1×10^{-5} in^2 to 1×10^{-4} in^2 in steps of 1×10^{-4} in^2, and allowable expected control effort (β^2) of 50 lb^2 to 80 lb^2 in steps of 10 lb^2 were used.

Table 1 summarizes the resulting minimum weight in pounds found for the case where a state-space realization based on the modal displacements and velocities was used. Intuitively, two trends would be expected in the data displayed in Table 1. The optimum weight should decrease as the allowable control effort β^2 is increased at constant allowable output response α^2 (left to right across the table), and the optimum weight should decrease as the allowable output response α^2 is increased at constant allowable control effort β^2 (down the table). With reference to Table 1, we can see that this trend is observed in a macroscopic sense only, there being several examples where this trend is not observed. For example, considering the first column of Table 1, which corresponds to $\beta^2 = 50$ lb^2 for varying α^2, we see only two exceptions to the expected trends, these being at α^2 values of 6×10^{-5} and 9×10^{-5}. Similar results are observed in all other columns and rows of Table 1. Results obtained using a state-space realization based on the physical displacements and velocities of nodal points are more consistent than when using the modal variables, although still not totally uniform. It might be pointed out that the results when using a physical realization were consistently easier to obtain, there being no need to alter the nominal value of γ_{min} to obtain convergence, and the number of global iterations required for convergence being consistenty lower.

Some understanding of these contradictory results can be found by considering Table 2, which gives the optimal element areas found for $\beta^2 = 50$ and for the varying α^2 corresponding to the first column of Table 1. Also given in this table is the number of global iterations required for convergence, the final values of the Lagrange multipliers (which then defines the LQR controller), and the initial value of the structural design variables (all the same for the symmetric set of initial conditions) at which the initial scaled system satisfies the constraints. Immediately apparent from Table 2 is a number of seemingly separate regions of the design space into which this structure has converged. For example, the final designs for $\alpha^2 = 5 \times 10^{-5}$ and $\alpha^2 = 7 \times 10^{-5}$ seem to be similar in relative structure. Here, "similar" refers to the relative sizing of the structural members, in that design variables that are "larger" in one design are "larger" in the other. Both these designs are however distinctly different from those for $\alpha^2 = 1 \times 10^{-5}$ and $\alpha^2 = 3 \times 10^{-5}$, which themselves are similar. The conclusion seems to be that we are converging into different regions of the design space with our solution algorithm, and that there are numerous local minima. Several columns of Table 2 seem to define their own region of the design space, being dissimilar to any other column. In other words, our design space seems to have multidimensional corrugations leading to multiple local minima. The solutions will lie somewhere on the intersection hyperplane between the surface of constant allowable output response and the surface of constant allowable control effort.

This corrugated nature of the design space can be illustrated by considering the solutions obtained, for the same constraint case, when starting from different initial conditions. For the case of $\beta^2 = 75$ and $\alpha^2 = 1 \times 10^{-5}$, Table 3 summarizes the results of runs made when modal state space realizations were used, and when only the initial conditions are varied. The different initial conditions are defined by setting all structural elements equal except the first (element 1), to which is added a percentage of the size of other elements. Even with this limited variation in the initial conditions, there are seemingly many distinct regions in the design space into which the system may converge. A picture of the constraint surfaces as a one-dimensional slice of the multidimensional space will emerge if these optimal structures are varied into each other in a linear fashion, and the constraint values are calculated between each case. That is, the structural design variables and Lagrange multipliers are changed linearly from the optimal values in one case to those in another case. Then the constraint surfaces obtained would be those seen when travelling in a straight line between each successive point.

The results of such an analysis are shown in Figures 3 for the cases corresponding to those given in Table 3. As expected, the weight varies linearly between the cases, but it is the constraint curves that are much more revealing. For example, considering Figure 3, one can see that between case 1 and case 2, there is a "ridge" of output response larger than the maximum allowable value. Similarly, the control effort first decreases, then also increases to a ridge of high value. This corresponds to a hump in the constraint surfaces between the two

points in the design space. Assuming that we would see such behaviour when moving in every direction away from case 1 and case 2, rather than just in a direction between the two as shown in Figure 3, then the design points corresponding to these cases would represent local minima. In this situation, the design can become "trapped" in such a locally convex region, causing the solution algorithm to converge to different points.

With reference to the same Figure 3, one can see that both the output response and control efforts are virtually constant between cases 2 and 3, while the weight increases slightly from 2053.0 lb to 2090.6 lb. This indicates that case 2 and case 3 actually represent the same optimal solution, with the difference being accounted for in the variance allowed by the convergence criteria used. The direction in the design space represented by the movement from case 2 to case 3 would lie in the intersection hyperplane of the surfaces of constant control effort and output response constraints, and would be at a shallow angle to the linear surface of constant weight. Figure 3 graphically illustrates a design space that is a very complicated function of the design variables, in which multiple local minima abound.

There are some other tests that can be made on the hypothesis that the design is becoming trapped in local minima. If the design is actually trapped in a local minimum, the solution should stay in the vicinity of that minimum if the problem is changed only slightly. That is, if a converged solution is used as the initial conditions for an optimization run where the constraint objectives are changed by a "small" amount, then the new problem should converge to a point that is "close to" the initial point. Table 4 represents such a situation. Here, the solution was first obtained for the case where $\beta^2 = 50$ and $\alpha^2 = 1 \times 10^{-5}$, and where a modal state space realization and inverse design variable approximations were used. This converged solution was then used as the initial conditions for the cases $\beta^2 = 50$ and $\alpha^2 = 2 \times 10^{-5}$, and $\beta^2 = 60$ and $\alpha^2 = 1 \times 10^{-5}$. Moving down each column, and across the top row, of Table 4, the converged solution from the previous case was used as the initial condition for the new problem. As can be seen from Table 4, the two expected trends in the data, as mentioned previously, are now observed without exception. The optimal solutions for the first column of Table 4, corresponding to the cases where $\beta^2 = 50$, are given in Table 5 The solutions now appear to be in the same local region of the design space, as evidenced by the relative sizing of the optimal structures. For example, note that in all converged designs, structural elements 9, 10, and 12 are at their lower gage limit of 0.1 in^2, and that the first structural element is the largest by far. The optimal solutions for the $\beta^2 = 60$ cases from Table 4 also appear to be in this same region of the design space. These results test the hypothesis that designs are converging to local minima, and indicate that the local optima are real and not simply figments of a numerical imagination.

5.2 Direct Output Feedback Control

Recall that when using direct output feedback, no simplifying assumptions can be made regarding the controller design variables (elements of K), such as the LQR assumption used in the case of full state feedback. Therefore, no scaling of the structure and controller to the closest constraint surface is performed. If a full state feedback case is to be solved in the form of direct output feedback with $H = I$, the number of design variables will increase significantly over the number of design variables created when other types of controllers are considered. This is because the number of states in the plant model will generally be large for anything but trivial systems, hence K will have many elements, all of which will be treated explicitly as design variables. However, such a situation is considered here to aid a comparison between the two solution algorithms, and the results obtained in the previous section. For the continuation algorithm, convergence was obtained after the specified number of global iterations, set by the specification of $\Delta\gamma$. Also note that, since only one each of the output response and control effort constraints are specified at this stage ($n_\alpha = 1$, $n_\beta = 1$), these can both be set as equality constraints without loss of generality since they will both be active at an optimum.

Table 6 gives the optimal weights found using the sequential approximations solution algorithm in the case when a physical state space realization and inverse design variable approximations are used, for $\beta^2 = 50$ and $\beta^2 = 60$, and for varying α^2. Compared to the similar case when scaling was performed, the optimal weights found here are larger in every case. Additionally, the solution times were significantly larger because of the number of iterations required for convergence. Note that some values in Table 6 are for situations where an average steady state value was obtained, but where the design was jumping around too much over each global iteration for convergence to occur. This was so even though the move-limits for every case in Table 6 were set at a relatively small $\pm 2.5\%$. A smaller move-limit would aid convergence, but slow it considerably. Also, smaller move-limits may cause premature convergence if the design is at a point where the constraint surfaces

and the surface of constant weight are nearly parallel.

Table 7 gives the optimal weights found using the continuation algorithm for the same cases listed in Table 6. All cases listed were obtained with the continuation parameter $\Delta\gamma = 0.01$ until $\gamma = 0.5$, when $\Delta\gamma$ became 0.02, so that for every case convergence was achieved in 75 global iterations. Also listed in Table 7 are the move-limits on the maximum parameter changes allowable locally (ϵ in Section 3.2). These are set to give a tradeoff between the satisfaction of the local linearity assumption and convergence to the local neigbouring problem, and must be found by numerical experimentation. Note that in both situations represented by Tables 6 and 7, minimum move-limits on the elements of K are set so that these elements can change sign if desired.

The solutions given in Tables 6 and 7 were obtained when the initial structure was defined with all truss elements of equal cross-sectional area. The particular values for this area are given in Tables 6 and 7 for each case, and were chosen so that the initial output response was "close to" its desired final value. With all structural elements at 120 in^2, 90.0 in^2, and 60.0 in^2, the initial output responses were 2.067×10^{-5}, 3.674×10^{-5}, and 8.266×10^{-5} respectively. The initial control effort was zero of course, since all elements of K were set initially to zero.

Comparing the optimal weights from Tables 6 and 7, it can be seen that those obtained using the continuation solution algorithm are significantly lower than those obtained using the sequential approximations solution algorithm in every case. The optimal weights are also much more consistent, in terms of the expected trends as α^2 increases, when using the continuation method. Convergence was obtained for every case listed in Table 7, whereas for three of the cases listed in Table 6, no convergence was obtained within 300 iterations. The reason for the convergence failure can be illustrated by considering the convergence histories given in Figures 4 and 5, for typical cases from Tables 6 and 7 respectively. The inset in Figure 4 shows some of the histories toward the end of the solution in more detail. These can be seen to be very rough, as compared to the histories in Figure 5 which are smooth everywhere. These parameter oscillations for the sequential approximations solution technique are indicative of a move-limit set too high, so that the local linearity assumption is violated. However, since the convergence is very flat toward the end of the solutions, a smaller move-limit is likely to cause premature convergence, or to significantly slow down the convergence for very little additional objective reduction.

The optimal weights found using the continuation method listed in Table 7 compare very favourably with those found for the same cases ($\beta^2 = 50$ and varying α^2) when the full state feedback LQR assumption was used to simplify solution. In almost every case, the optimal weight is approximately equal to or lower than those found earlier. However, the sequential approximations solution algorithm results are much worse, being significantly larger than the optimal weights found earlier in every case. The sequential approximations solution algorithm performs so poorly because it tends to become trapped in a local minimum close to the specified initial conditions.

Consider now cases where the full state is not available for feedback. In the DRAPER I structure, the six right-angled bipods are usually assumed to take on the duties of force actuators and colocated rate sensors, so that $H = G^T$ (output state of dimension six). Tables 8 and 9 list the optimal weights found for this reduced-order output vector for the same cases used in Table 6, when the sequential approximations and continuation solution algorithms respectively are used. Note that the optimal weights consistently obey the trends that are expected as the allowable output response and controller effort are altered. Even so, the designs can converge into completely different regions of the design space for any particular case. This is illustrated by Table 10, which gives the optimal structural design variables for the cases represented by the second column of Table 9. Note that every solution does not define a unique local minima. Many of the solutions seem to lie in the same local minima region, for example the solution for the case $\alpha^2 = 1{,}7$, and 9×10^{-5}. Once again, the design space is found to have many local minima.

The two solution algorithms here seem to predict quite similar optimal weights for the cases considered, although in general those found using the continuation method are slightly better. However, convergence for the results using the sequential approximations solution algorithm were more difficult to obtain than those for the continuation method. Altering the nominal move limits (set at $\pm 2.5\%$), and perhaps reducing it toward the latter stages of each solution would aid convergence, but at increased effort on the part of the user. The continuation results are easier to obtain since they require less individualized attention.

Comparing Tables 8 and 9 to Table 7, it can be seen that the optimal weights found when $H = G^T$ are much larger than those found when full state feedback was used. The reason for this is the particular placement of the disturbance forces relative to the design output states (which determine the output response). For the

case considered here, the DRAPER I structure is disturbed at node 1, the displacement of which is to be kept below the design objective value α^2. With full state feedback, the displacement states of node 1 are available for feedback, whereas if $H = G^T$, these states are not available, and the effect of the displacement of node 1 is available only indirectly through its effect on the velocities along the six bipods that make up the sensors. The importance of these states can be seen by examining the optimal gain matrices for the full state feedback case. The largest gains associated with displacements and velocities in these matrices appear in the columns corresponding to node 1 degrees of freedom, indicating that the states associated with node 1 are very important. When they are not available, the controller does not have as much information about the state of node 1, the node it is trying to control, as it does in the case of full state feedback, and will increase the structural stiffness (and hence mass) to compensate.

To illustrate further, consider output feedback with the displacement and velocity states of node 1 added to the output vector used previously. The optimal weights for the same $\beta^2 = 50$ and $\beta^2 = 60$ cases used in Table 9 with this new output vector (of dimension 12 now) are given in Tables 11 and 12, when the sequential approximations and continuation solution algorithms are used respectively. There are now larger differences between the weights found using the two solution algorithms than in the case when $H = G^T$ only, with the continuation method giving the best results (with one exception). The weights obtained using the continuation algorithm are now very close to those obtained when using full state feedback (in Table 7), although still a little larger in every case. This is because even with this larger output vector, the displacement states for nodes two through four are still not used in the controller.

All the results presented so far were generated with the external stochastic disturbance intensities set at one ($X_w = I$). If these intensities are varied as $X_w = x_w I$, the effect of varying x_w on the optimal weight is shown in Figure 6. These results were generated using the continuation solution algorithm, for the case when $\alpha^2 = 1 \times 10^{-5}$ and $\beta^2 = 50$, and when all structural design variables were initially set at 120 in^2. As can be seen, the relationship between the disturbance intensity and the optimal structural weight appears basically linear in the range shown. However, a linear fit of the data does not produce an optimum weight of zero for a zero intensity disturbance, as would be expected. Therefore, the relationship cannot be exactly linear. The results also indicate that the disturbance level chosen for the previous results ($x_w = 1$) was significant for the range of output response and control effort constraint objectives used.

As long as the neighbouring problems in the continuation algorithm were close enough, which was satisfied by starting from an initial point where the constraint values were "close to" their final desired locations, no difficulties were experienced in obtaining convergence. The solution times for the continuation algorithm were 2–3 times longer than for solutions by the sequential approximations algorithm, since on average approximately 8–12 local iterations were required for convergence to the neighbouring problem for each global iteration. The performance of the sequential approximations solution algorithm decreases as the dimensionality increases, as evidenced by the sequence of cases where $H = G^T$ (48 design variables), $H = G^T$ plus node 1 displacement and velocity states (84 design variables), and $H = I$ (156 design variables). However, the continuation method seemed much less sensitive to the problem dimension. The continuation solution method was found to be generally superior, for this problem at least, to the sequential approximations solution method, with respect to the confidence in obtaining a "good" converged solution. The disparity in solution times was acceptable because of the ease with which solutions were obtained using the continuation method, and because the solutions found seemed to be generally much better than those found using the sequential approximations algorithm.

6 Conclusions

In this work, the integrated control/structure design optimization problem has been investigated from a response to disturbances point of view. Both full state and output feedback controllers were employed in the control strategy, and two solution methods were compared. It was found that for this problem, the continuation method coupled with a sequential linear programming approach performed better than the more traditional type of nonlinear approximations approach, in the sense that it was more robust to changes in the arbitrary parameters set by the user, obtained better results, and the results were easier to obtain. The design space was found to exhibit multiple local minima in which the solution could become trapped, although the continuation solution method seemed to handle the corrugated design space better than the other method. In future work, more diverse controller types must be considered, along with structures consisting of more complicated finite

elements than simple truss members. Additionally, more realistic problems of higher dimension must be solved, to demonstrate the practicality of this design procedure.

Acknowledgments

This work was partially funded by the Air Force Office of Sponsored Research at the Flight Dynamics Laboratory, Wright Aeronautical Laboratiories, and also by a grant from CRAY Research Inc. Computer facilities on a CRAY-XMP were provided by the Ohio Supercomputer Center in Columbus, Ohio.

References

[1] Hanks, B.R. and Skelton, R.E., "Designing Structures for Reduced Response by Modern Control Theory", Proceedings of the 24th AIAA Structures, Structural Dynamics and Materials Conference, Lake Tahoe, Nevada, May 2–4, 1983.

[2] Komkov, V., "Simultaneous Control and Optimization for Elastic Systems", Proceedings of the Workshop on Applications of Distributed System Theory to the Control of Large Space Structures, JPL Publication 83-46, ed. by G. Rodriguez, July 1983.

[3] Hale, A.L., Lisowski, R.J. and Dahl, W.E., "Optimizing Both the Structure and the Control of Maneuvering Flexible Structures", Proceedings of the AAS/AIAA Astrodynamics Conference, Lake Placid, New York, August 22–24, 1983.

[4] Salama, M., Hamidi, M. and Demsetz, L., "Optimization of Controlled Structures", Proceedings of the JPL Workshop on Identification and Control of Flexible Space Structures, San Diego, California, June 4–6, 1984.

[5] Messac, A., Turner, J. and Soosaar, K., "An Integrated Control and Minimum Mass Structural Optimization Algorithm for Large Space Structures", Proceedings of the JPL Workshop on Identification and Control of Flexible Space Structures, San Diego, California, June 4–6, 1984.

[6] Miller, D.F. and Shim, J., "Gradient Based Combined Structural and Control Optimization", *J. Guidance and Control*, Vol. 10, No. 3, May–June 1987, pp 291–298.

[7] Onoda, Junjiro and Haftka, Raphael T., "Simultaneous Structure/ Control Optimization of Large Flexible Spacecraft", AIAA paper 87-0823.

[8] Slater, G.L., "A Disturbance Model for the Optimization of Control/Structure Interactions for Flexible Dynamic Systems", AIAA Guidance, Navigation and Control Conference, Minneapolis MN, August 15–17, 1988, pp 57–63; AIAA Paper 88-4058-CP.

[9] Khot, N.S., Eastep, F.E. and Venkayya, V.B., "Simultaneous Optimal Structural/Control Modifications to Enhance the Vibration Control of a Large Flexible Structure", Proceedings of the AIAA Guidance, Navigation and Control Conference, Snowmass, CO, Aug. 19–21, 1985, pp 459–466.

[10] Khot, N.S., "Minimum Weight and Optimal Control Design of Space Structures", NATO Advanced Study Institute, Computer Aided Optimal Design: Structural and Mechanical Systems, Troia, Portugal, June 29–July 11, 1986.

[11] Schmit, L.A., and Farshi, B., "Some Approximation Concepts for Efficient Structural Synthesis",*AIAA Journal*, Vol. 12, No. 5, 1974, pp 692–699.

[12] Grandhi, R.V. and Venkayya, V.B., "Structural Optimization with Frequency Constraints", *AIAA Journal*, Vol 26, No. 7, July 1988, pp 858–866.

[13] Slater, G.L. and Kandadai, R.D., "Gain Optimization with Non-Linear Controls", *Optimal Control Applications and Methods*, Vol. 5, pp 207–219, 1984.

[14] Starnes, J.H. Jr. and Haftka, R.T., "Preliminary Design of Composite Wings for Buckling, Strength and Displacement Constraints", *Journal of Aircraft*, Vol. 16, No. 8, August 1979, pp 564–570.

[15] Kirk, D.E., *Optimal Control Theory, An Introduction*, Prentice-Hall, Englewood Cliffs, New Jersey, 1970.

[16] Canfield, R.A., Grandhi, R.V. and Venkayya, V.B., "Comparison of Optimization Algorithms for Large Structures", Report AFWAL-TM-86-204-FIBR, Wright-Patterson Air Force Base, May 1986.

[17] Lim, K.B. and Junkins, J.L., "Robustness Optimization of Structural and Controller Parameters", *J. Guidance, Control and Dynamics*, Vol. 12, No. 1, Jan.–Feb. 1989, pp 89–96.

[18] Horta, L.G., Juang, J-N. and Junkins, J.L., "A Sequential Linear Optimization Approach for Controller Design", *J. Guidance, Control and Dynamics*, Vol. 9, No. 6, Nov.–Dec. 1986, pp 699–703.

[19] Strunce, R., Lin, J., Hegg, D and Henderson, T., "Actively Controlled Structures Theory", Final Report, Vol 2 of 3, R-1338, Charles Stark Draper Laboratory, Cambridge, Mass. Dec. 1979.

[20] McLaren, M.D., "Controller Methodologies for the Integrated Control/Structure Design Optimization of Large Flexible Structures", Ph.D. Dissertation, University of Cincinnati, December 1989.

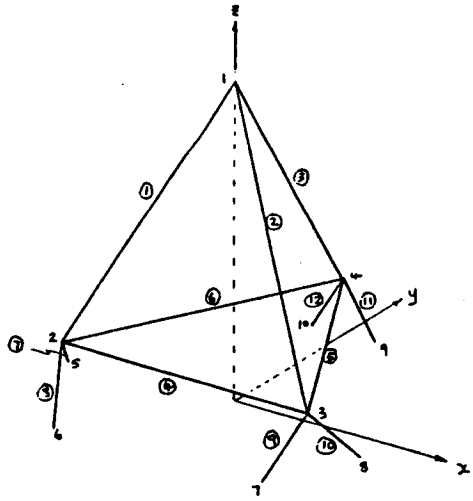

Figure 1: The DRAPER I Structure

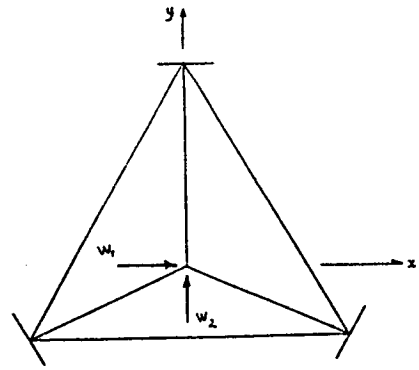

Figure 2: The disturbance model

α^2 ($\times 10^{-5}$)	β^2			
	50	60	70	80
1	2847.1	2991.4	2107.4	2924.9
2	2077.3	2030.8	1914.4	1289.7
3	1878.0	1658.9	1472.9	1216.8
4	1548.3	1409.7	1653.2	1021.5
5	1418.9	1319.2	1459.5	937.4
6	1460.6	1209.5	964.9	1009.8
7	1209.0	1076.0	928.7	1052.7
8	1066.7	1214.1	987.9	790.2
9	1126.3	940.5	854.0	720.1
10	971.9	1035.1	766.4	970.6

Table 1: Optimal weight using a modal state-space realization, the symmetric set of initial conditions, and inverse design variable approximations.

	α^2 ($\times 10^{-5}$)				
	1	2	3	4	5
Scaled DV	90.437	63.947	52.212	45.213	40.441
Final DV					
1	125.893	73.091	70.557	49.717	43.868
2	23.336	53.545	36.664	21.137	23.151
3	45.632	15.268	14.833	35.217	21.510
4	6.389	10.704	5.599	6.318	4.957
5	10.973	5.375	12.207	4.213	9.637
6	9.800	6.209	6.953	5.365	4.914
7	17.627	8.610	10.775	5.638	9.310
8	17.719	0.124	8.802	0.150	9.901
9	0.100	13.250	0.100	0.100	0.100
10	0.100	9.332	0.711	0.313	8.307
11	18.206	0.100	13.746	9.473	8.352
12	0.100	0.100	0.100	9.266	0.100
λ_u	1.6710	1.4574	1.2620	1.4851	0.8632
λ_y	1.0	1.0	1.0	1.0	1.0
iter. for convergence	44	19	15	32	32

	α^2 ($\times 10^{-5}$)				
	6	7	8	9	10
Scaled DV	36.918	34.180	31.973	29.979	28.594
Final DV					
1	25.936	32.194	9.723	16.757	20.331
2	30.650	21.255	27.425	32.495	38.508
3	28.247	20.736	28.618	16.565	11.434
4	11.168	5.141	4.083	8.798	2.041
5	10.922	7.713	6.737	4.348	2.369
6	6.795	4.260	3.815	6.692	2.934
7	0.101	8.299	0.100	0.100	0.152
8	2.501	9.363	0.100	9.628	0.885
9	0.245	0.100	6.482	1.332	3.242
10	9.107	8.183	8.323	0.100	5.016
11	7.744	7.379	8.218	7.737	2.532
12	8.583	0.100	6.782	10.099	0.100
λ_u	0.7522	0.8544	0.7937	0.9117	1.7622
λ_y	1.0	1.0	1.0	1.0	1.0
iter. for convergence	21	18	22	22	49

Table 2: Optimal design variables for $\beta^2 = 50$

	Case 1	Case 2	Case 3	Case 4	Case 5
Final Wt.	2451.3	2053.0	2090.6	1915.6	2067.0
Final DV					
1	73.849	41.076	55.595	38.306	60.319
2	70.699	49.211	55.391	68.734	48.760
3	13.262	74.820	58.403	44.107	50.104
4	16.100	2.146	1.6065	1.227	2.841
5	7.730	1.843	1.4806	1.612	2.169
6	8.068	1.819	1.5676	3.161	2.834
7	3.864	0.100	0.100	0.100	0.170
8	20.163	0.100	0.100	0.451	0.100
9	21.568	0.100	0.100	7.939	8.984
10	5.694	0.100	0.100	0.100	0.100
11	0.100	0.100	0.100	0.100	0.100
12	0.100	0.100	0.100	0.100	9.014
λ_u	0.9765	3.1055	3.3391	2.6755	2.5236

For all $j \neq 1$, the initial conditions are:
Case 1: $p_1 = p_j$
Case 2: $p_1 = p_j + 3\%$
Case 3: $p_1 = p_j + 6\%$
Case 4: $p_1 = p_j + 10\%$
Case 5: $p_1 = p_j + 50\%$

For all cases, $(\lambda_u)_0 = 1.0$, $(\lambda_y)_0 = 1.0$

Table 3: Optimal values when $\beta^2 = 75$ and $\alpha^2 = 1 \times 10^{-5}$ for differing initial conditions, when using a modal state space model

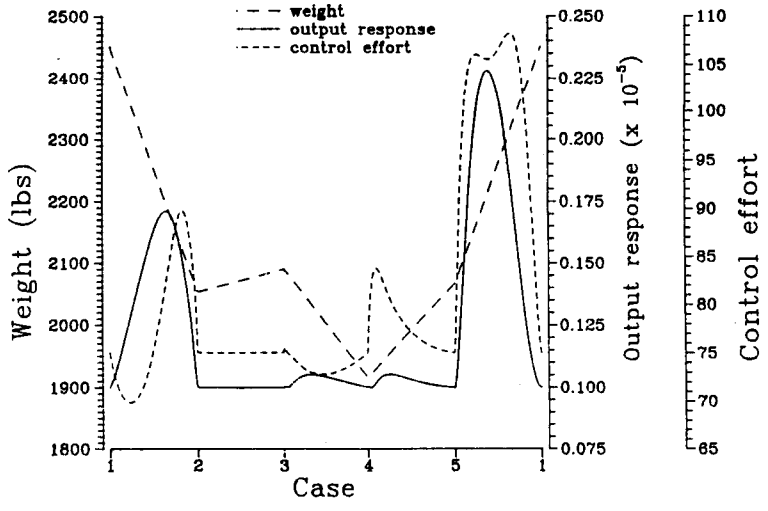

Figure 3: Constraint surfaces between cases listed in Table 3

α^2 ($\times 10^{-5}$)	β^2			
	50	60	70	80
1	2847.1	2466.0	2166.6	1969.2
2	2045.9	1782.1	1579.7	1443.2
3	1685.6	1478.8	1327.5	1197.2
4	1470.9	1298.0	1162.0	1052.0
5	1325.2	1174.2	1049.3	952.1
6	1217.0	1083.2	965.9	880.0
7	1134.1	1012.4	901.4	823.8
8	1065.7	955.3	849.4	776.5
9	1014.5	907.9	806.4	735.3
10	961.3	861.0	770.0	700.2

Table 1: Optimal weight using a modal state-space realization and inverse design variable approximations, where the initial condition for each case is the converged solution from the previous case.

α^2 ($\times 10^{-5}$)	initial dv's (structural)	optimal weight		iterations	
		$\beta^2 = 50$	$\beta^2 = 60$	$\beta^2 = 50$	$\beta^2 = 60$
1	120.0	3847.9	3548.4	220	300*
2	90.0	2724.3	2490.7	202	300*
3	90.0	2191.7	2083.1	231	300*
4	90.0	1950.8	1771.3	188	300*
5	90.0	1680.5	1702.5	300*	181
6	90.0	1529.7	1443.9	300*	300*
7	60.0	1443.0	1395.0	207	181
8	60.0	1325.6	1247.4	300*	300*
9	60.0	1688.2	1591.6	119	123
10	60.0	1604.4	1487.0	126	127

* indicates no convergence in specified number of global iterations

Table 6: Optimal weight using sequential appproximations solution algorithm without scaling for full state feedback, a physical state-space realization, and inverse design variable approximations.

α^2 ($\times 10^{-5}$)	initial dv's (structural)	optimal weight	
		β^2=50	$\beta^2 = 60$
1	120.0	3255.6	3013.7
2	90.0	2291.0	2116.4
3	90.0	1864.9	1737.2
4	90.0	1617.7	1630.3
5	90.0	1450.0	1447.6
6	90.0	1321.6	1221.0
7	60.0	1226.8	1135.0
8	60.0	1143.9	1064.0
9	60.0	1085.4	1002.9
10	60.0	1024.3	961.8

Table 7: Optimal weight using continuation solution algorithm without scaling for full state feedback, and a physical state-space realization.

α^2 ($\times 10^{-5}$)	initial dv's (structural)	β^2	
		50	60
1	120.0	4764.9	4502.3
2	90.0	3553.6	3170.5
3	90.0	2744.5	2586.7
4	90.0	2511.8	2388.8
5	90.0	2090.7	2004.6
6	90.0	1954.7	1830.1
7	60.0	1797.0	1698.4
8	60.0	1683.6	1585.0
9	60.0	1584.3	1496.5
10	60.0	1503.4	1420.1

Table 9: Optimal weight using continuation solution algorithm for direct output feedback with $H = G^T$, and a physical state space realiza-

	α^2 ($\times 10^{-5}$)				
	1	2	3	4	5
Final DV					
1	125.893	82.406	66.777	57.864	50.877
2	23.336	19.075	16.010	14.170	13.257
3	45.632	36.194	29.987	26.286	23.752
4	6.389	6.372	5.386	4.736	4.105
5	10.973	8.135	6.487	5.952	5.429
6	9.800	8.558	7.433	6.631	6.031
7	17.627	12.148	12.085	9.342	11.208
8	17.719	10.689	8.446	6.718	5.422
9	0.100	0.100	0.100	0.100	0.100
10	0.100	0.100	0.100	0.100	0.100
11	18.206	11.326	8.820	8.172	7.764
12	0.100	0.100	0.100	0.100	0.100
λ_u	1.6710	1.6281	1.6293	1.6325	1.6273
λ_y	1.0	1.0	1.0	1.0	1.0
iter. for convergence	44	16	2	2	2
	α^2 ($\times 10^{-5}$)				
	6	7	8	9	10
Final DV					
1	46.745	42.850	40.259	37.112	33.742
2	12.302	11.800	11.108	11.403	11.179
3	21.926	20.458	19.239	18.610	17.761
4	3.996	3.621	3.446	4.045	3.745
5	5.144	4.708	4.451	3.751	4.167
6	5.556	5.241	4.926	4.681	4.634
7	7.501	9.330	8.344	7.053	6.621
8	5.286	4.390	4.167	5.319	5.070
9	0.100	0.100	0.100	0.100	0.100
10	0.100	0.100	0.100	0.100	0.100
11	7.237	6.603	6.216	4.678	5.357
12	0.100	0.100	0.100	0.100	0.100
λ_u	1.6243	1.6163	1.6167	1.5670	1.5540
λ_y	1.0	1.0	1.0	1.0	1.0
iter. for convergence	2	2	2	4	3

Table 5: Optimal design variables for $\beta^2 = 50$ cases given in Table 4

α^2 ($\times 10^{-5}$)	initial dv's (structural)	optimal weight		iterations	
		$\beta^2 = 50$	$\beta^2 = 60$	$\beta^2 = 50$	$\beta^2 = 60$
1	120.0	4830.5	4616.8	400*	400*
2	90.0	3626.9	3262.8	223	400*
3	90.0	2903.5	2668.4	400*	400*
4	90.0	2393.5	2324.4	400*	400*
5	90.0	2152.3	2054.5	290	400*
6	90.0	2067.1	1893.6	312	265
7	60.0	1811.6	1815.2	336	254
8	60.0	1704.1	1639.7	400*	400*
9	60.0	—	—	—	—
10	60.0	1629.4	1487.0	425	500*

* indicates no convergence in specified number of global iterations

Table 8: Optimal weight using sequential appproximations solution algorithm for direct output feedback with $H = G^T$, and a physical state-space realization.